Time Course of Discordant BMIPP and Thallium Uptake After Ischemia and Reperfusion in a Rat Model

Takahiro Higuchi, MD, PhD[1,2]; Junichi Taki, MD, PhD[2]; Kenichi Nakajima, MD, PhD[2]; Seigo Kinuya, MD, PhD[2]; Masanobu Namura, MD, PhD[3]; and Norihisa Tonami, MD, PhD[2]

[1]PET Center, Kanazawa Cardiovascular Hospital, Kanazawa, Japan; [2]Department of Biotracer Medicine, Kanazawa University Graduate School of Medical Sciences, Kanazawa, Japan; and [3]Department of Cardiology, Kanazawa Cardiovascular Hospital, Kanazawa, Japan

Serial changes in fatty acid metabolism or use associated with acute ischemia and reperfusion were examined in rat hearts. **Methods:** Male Wistar rats were subjected to occlusion of the left coronary artery for 20 min followed by reperfusion. After release of the occlusion, groups of animals were allowed to recover for intervals of 20 min ($n = 9$), 1 d ($n = 9$), 3 d ($n = 6$), 7 d ($n = 6$), or 30 d ($n = 6$). Hearts were excised 15–20 min after injection of 0.74 MBq of ^{125}I-15-(p-iodophenyl)-3-R,S-methylpentadecanoic acid (BMIPP) and 14.8 MBq of ^{201}Tl. One minute before resection, the left coronary artery was reoccluded and 185 MBq of ^{99m}Tc-sestamibi were injected to document the area at risk. Triple-tracer autoradiography was performed to assess tracer uptake. Uptake ratios of BMIPP and ^{201}Tl in the area at risk were calculated on the basis of the count density in the lesion divided by that in the normally perfused area. **Results:** ^{201}Tl uptake did not change throughout the observation period ($P = 0.25$). In contrast, BMIPP uptake increased early in the acute phase (20 min and 1 d), decreased during the subacute phase (7 d), and subsequently recovered in the chronic phase (30 d). **Conclusion:** The present investigation clearly illustrated that BMIPP uptake is higher than ^{201}Tl uptake in the acute phase, that BMIPP uptake is lower than ^{201}Tl uptake in the subacute phase, and that BMIPP uptake and ^{201}Tl uptake are similar in the chronic phase. These results yield data essential to the precise interpretation of BMIPP images.

Key Words: BMIPP; ischemia; reperfusion; fatty acid metabolism; autoradiography

J Nucl Med 2005; 46:172–175

Fatty acid metabolism is a major pathway of energy production in normally perfused myocardium; however, this process is impaired during and after events associated with myocardial ischemia and succeeding reperfusion. Therefore, evaluation of fatty acid metabolism yields important

data on myocardial conditions in ischemic heart disease (1–8).

15-(p-iodophenyl)-3-R,S-methylpentadecanoic acid (BMIPP) has been proposed as a fatty acid probe. The methyl-branched fatty acid analog displays rapid extraction and prolonged retention in the myocardium based on its resistance to β-oxidation (9–11). Discordant scintigraphic findings between ^{123}I-BMIPP and perfusion tracers such as ^{201}Tl, ^{99m}Tc-sestamibi, and ^{99m}Tc-tetrofosmin have been documented in patients with coronary artery disease (5,7,12–15). However, serial changes in acid metabolism assessed by BMIPP uptake from the acute phase to the chronic phase after ischemic events have not thoroughly been examined.

Therefore, the impact of brief intervals of total coronary artery occlusion and reperfusion on myocardial uptake of BMIPP was investigated for precise interpretation of scintigraphic findings involving BMIPP and comparison with ^{201}Tl uptake.

MATERIALS AND METHODS

Animal Model of Acute Ischemia and Reperfusion

Male Wistar rats (8–11 wk old) were anesthetized with intraperitoneal administration of 40 mg of pentobarbital per kilogram of body weight and ventilated mechanically with room air. After left thoracotomy and exposure of the heart, a 7-0 polypropylene suture on a small curved needle was passed through the myocardium beneath the proximal portion of the left coronary artery; subsequently, both ends of the suture were passed through a small vinyl tube, which produced a snare. The suture material was pulled tightly against the vinyl tube to occlude the left coronary artery for 20 min. Myocardial ischemia was confirmed by ST-segment elevation on electrocardiography and regional cyanosis of the myocardial surface. Reperfusion, which was obtained by release of the snare, was confirmed by the appearance of a myocardial blush over the area at risk. The snare remained loose on the surface of the heart for reocclusion in the 20-min reperfusion model. In the remaining animals, the snare was also left loose at the surface of the heart until repeated thoracotomy. At 20 min ($n = 9$), 1 d ($n = 9$), 3 d ($n = 6$), 7 d ($n = 6$), or 30 d ($n = 6$) after reperfusion (Fig. 1), 0.74 MBq of ^{125}I-BMIPP (Medi-Physics) and 14.8 MBq of ^{201}Tl (Daiich Radioisotope Laboratories) were injected via a tail
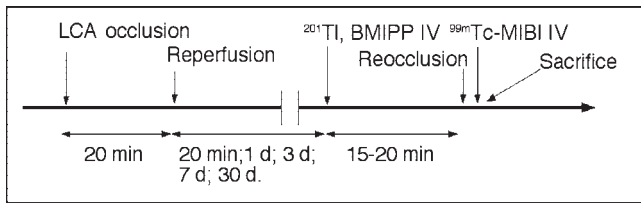
FIGURE 1. Schematic diagram illustrating protocol of ischemia and reperfusion in rat experimental model. After reperfusion, groups of animals were allowed to recover for various intervals ranging from 20 min to 30 d before tracer injection. MIBI = sestamibi.

vein. For delineation of the area at risk, the left coronary artery was reoccluded 15–20 min after administration of ^{125}I-BMIPP and ^{201}Tl; subsequently, 185 MBq of ^{99m}Tc-sestamibi (Daiich Radioisotope Laboratories) were injected. One minute later, the rat was euthanized and the heart was removed for analysis. The heart was rinsed in saline, frozen in isopentane, cooled in dry ice, and embedded in methylcellulose. Serial short-axis sections (20-μm thickness) of the heart were produced on a cryostat for autoradiography.

Triple-Tracer Autoradiography

Triple-tracer autoradiography of left ventricular short-axis slices was performed on BAS-MS imaging plates (Fuji Film) to assess ^{125}I-BMIPP and ^{201}Tl uptake and the ischemic area at risk (^{99m}Tc-sestamibi defect). The first autoradiographic exposure, for visualization of ^{99m}Tc-sestamibi distribution in order to image the area at risk at 1–2 h after sacrifice, was performed for 15–20 min. Three days later, the second exposure, for visualization of ^{201}Tl uptake, was performed for 6 h. Thirty days later, the third exposure, for visualization of BMIPP uptake, was performed for 1 wk.

Data Analysis

Tracer accumulation was evaluated in myocardial slices at the midventricular level and determined by analysis of digitized autoradiograms. Photostimulated luminescence in each pixel (100 × 100 μm) was measured with a bioimaging analyzer (BAS-5000; Fuji Film). For quantitative analysis, uptake values of each region of interest were expressed as photostimulated luminescence per unit area (1 mm^2) after the background correction. A background region of interest was set adjacent to the left ventricle. Ischemic and normally perfused areas were defined from the ^{99m}Tc-sestamibi image; moreover, these regions of interest were applied to the ^{125}I-BMIPP and ^{201}Tl images to assess uptake of these tracers. The uptake ratio in the area at risk was calculated by dividing the uptake value of the ischemic area by that of the normally perfused area.

Statistical Analysis

All results were expressed as mean ± SD. Statistical analyses were conducted on a Macintosh personal computer (Apple Computer, Inc.) with StatView 5.0 software (SAS Institute Inc.). The paired t test was used to analyze the difference in uptake ratios between ^{125}I-BMIPP and [201]Tl. Multiple group comparisons were performed using ANOVA, followed by the Scheffé test to identify differences among groups. A value of $P < 0.05$ was considered statistically significant.

RESULTS

Serial changes in ^{201}Tl and ^{125}I-BMIPP uptake, expressed as ratios to the unaffected area, after left coronary artery occlusion and reperfusion are summarized in Figure 2. Representative images are presented in Figure 3. [201]Tl uptake in the area at risk tended to decrease at 3–7 d after reperfusion but not statistically significantly throughout the observation period ($P = 0.25$). In contrast, distinct changes were noted in BMIPP uptake ($P < 0.001$): BMIPP uptake in the area at risk transiently increased in the acute phase (20 min and 1 d), decreased in the subacute phase (3 and 7 d), and recovered in the chronic phase (30 d). Consequently, discordant BMIPP and ^{201}Tl uptakes were obvious in the acute and subacute phases (Fig. 2). The higher ratio of BMIPP to ^{201}Tl in the acute phase was inverted in the subacute phase. In the chronic phase, uptake of the 2 tracers concordantly recovered to the baseline value.

DISCUSSION

The present study demonstrated time-dependent metabolic changes in the so-called area at risk. Changes occurring in the acute phase (20 min and 1 d) through the chronic phase (30 d) were clarified: First, in the acute phase, BMIPP uptake was enhanced significantly in the area at risk; second, uptake declined in the subacute phase; and third, uptake was subsequently restored to the baseline level in the chronic phase. In contrast, changes in perfusion were minimal from the acute phase to the chronic phase. Therefore, distinct mismatches between perfusion and metabolism
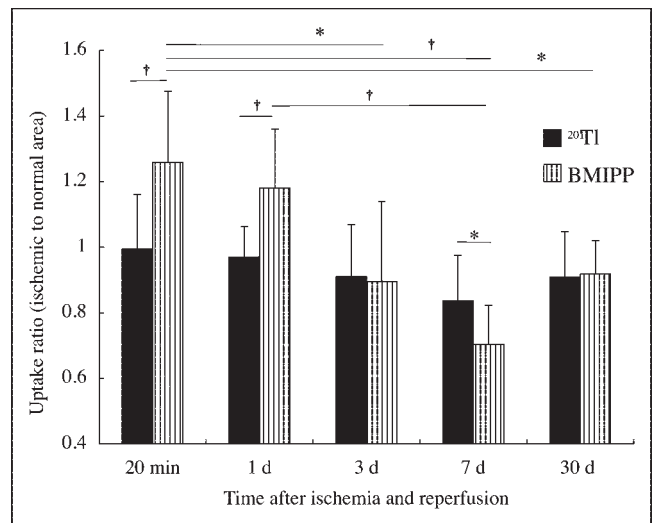

FIGURE 2. [201]Tl and BMIPP uptake ratios calculated by stimulated luminescence in area at risk divided by that in normally perfused areas. [201]Tl uptake ratios did not change significantly after reperfusion. However, BMIPP uptake ratios were affected markedly in a time-dependent fashion. When these 2 tracers were compared at the same time point, BMIPP uptake ratios were higher than ^{201}Tl uptake ratios at 20 min and 1 d and lower at 7 d after ischemia and reperfusion. *$P < 0.05$. †$P < 0.001$.
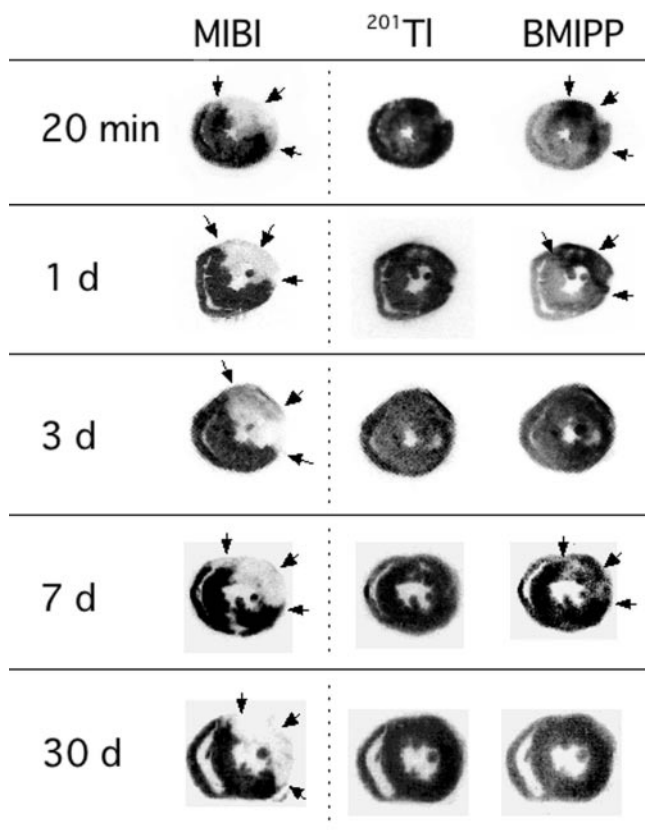
FIGURE 3. Autoradiograms of hearts of rats. BMIPP was injected at 20 min and at 1, 3, 7, and 30 d after the 20-min occlusion and reperfusion of left coronary artery. Midventricular slices serve as representatives for each group. ^{99m}Tc-Sestamibi defects demonstrate area at risk (indicated by arrows in the left column). ^{201}Tl uptake (middle column) in area at risk is relatively unchanged in comparison with that in unaffected area. In contrast, BMIPP uptake increases at 20 min and at 1 d (arrows), decreases at 7 d (arrows), and subsequently recovers at 30 d (right column). MIBI = sestamibi.

were observed in the area at risk in the acute and subacute phases.

Free fatty acid is a major myocardial energy source involving β-oxidation after the tricarboxylic acid cycle in the basal oxygen state. BMIPP is a methyl-branched fatty acid analog designed to resist β-oxidation (*9*). Although a minor metabolic pathway involving α-oxidation and subsequent β-oxidation exists, most injected BMIPP is transported into myocytes, followed by adenosine triphosphate (ATP)–dependent activation to coenzyme A; subsequently, substantial quantities of BMIPP are esterified and retained in the triglyceride pool (*10,11,16,17*). Therefore, the myocardial BMIPP image is related predominantly to the triglyceride pool. Ischemic insult is known to increase the size of the triglyceride pool early after myocardial ischemia. Consequently, elevated BMIPP uptake observed in the acute phase should be a reflection of increased capacity of the triglyceride pool (*18,19*).

Under ischemic conditions, β-oxidation is suppressed by augmentation of glucose use; as a result, ATP levels in the myocardium decrease immediately. The ATP reduction influences the ATP-dependent process of conversion to BMIPP–coenzyme A, leading to an increase in inactivated BMIPP, which is returned to the circulation via diffusion (*12,13,20*). These metabolic abnormalities persist even after perfusion recovery, which was likely related to the reduced BMIPP uptake in the subacute phase observed in the current investigation.

Triple-tracer autoradiography using ^{125}I-BMIPP, ^{201}Tl, and ^{99m}Tc-sestamibi was conducted to assess fatty acid metabolism, to assess fatty acid perfusion, and to determine the area at risk, respectively. Based on differential tracer doses and physical half-lives of radionuclides, myocardial radioactivity deriving from ^{201}Tl and ^{125}I-BMIPP was approximately 100 times greater than that of other tracers at the time of autoradiographic exposure: at 3 and 30 d after preparation of sections for ^{201}Tl and ^{125}I-BMIPP, respectively. Therefore, the contribution of cross-talk to each image was negligible.

^{201}Tl is known to redistribute gradually, but the 15- to 20-min interval between ^{201}Tl injection and sacrifice is relatively short for redistribution. Therefore, those images may reflect mainly myocardium perfusion.

A ^{123}I-labeled BMIPP SPECT technique is available in clinical settings for evaluation of various cardiac diseases (*21–27*). Discordance between BMIPP uptake and perfusion tracer uptake is associated with such conditions as revascularization after acute myocardial infarction (*21,22*). In many cases characterized by discordant tracer uptake, BMIPP uptake is typically lower than perfusion tracer uptake. However, higher BMIPP uptake is occasionally observed (*27*). The current findings suggested that the time after an ischemic event significantly affects BMIPP uptake in the area at risk; that is, enhanced uptake is evident in the acute phase, followed by a decrease in the subacute phase and subsequent recovery in the chronic phase. In clinical examinations, these findings could contribute to the interpretation of images obtained at various intervals after the ischemic event. At the same time, more clinical investigations are required to validate these rat-model findings so that they can be applied to clinical situations.

CONCLUSION

BMIPP uptake in the area at risk displayed time-dependent changes after an ischemic event and reperfusion in a rat experimental model. BMIPP uptake increased in the acute phase, followed by a decrease in the subacute phase and subsequent recovery in the chronic phase. These changes were independent of perfusion tracer uptake. In consequence, we observed BMIPP uptake higher than ^{201}Tl uptake in the acute phase and lower than ^{201}Tl uptake in the subacute phase, followed by similar BMIPP and ^{201}Tl uptakes in the chronic phase. These results may contribute to the precise interpretation of BMIPP images.

REFERENCES

1. Schwaiger M, Hicks R. The clinical role of metabolic imaging of the heart by positron emission tomography. *J Nucl Med.* 1991;32:565–578.

2. Schwaiger M, Schelbert HR, Ellison D, et al. Sustained regional abnormalities in cardiac metabolism after transient ischemia in the chronic dog model. *J Am Coll Cardiol.* 1985;6:336–347.

3. Schelbert HR, Henze E, Keen R, et al. C-11 palmitate for the noninvasive evaluation of regional myocardial fatty acid metabolism with positron-computed tomography. IV. In vivo evaluation of acute demand-induced ischemia in dogs. *Am Heart J.* 1983;106:736–750.

4. Liedtke AJ. Alterations of carbohydrate and lipid metabolism in the acutely ischemic heart. *Prog Cardiovasc Dis.* 1981;23:321–336.

5. Taki J, Nakajima K, Matsunari I, et al. Assessment of improvement of myocardial fatty acid uptake and function after revascularization using iodine-123-BMIPP. *J Nucl Med.* 1997;38:1503–1510.

6. Matsunari I, Saga T, Taki J, et al. Improved myocardial fatty acid utilization after percutaneous transluminal coronary angioplasty. *J Nucl Med.* 1995;36:1605–1607.

7. Franken PR, Dendale P, De Geeter F, Demoor D, Bossuyt A, Block P. Prediction of functional outcome after myocardial infarction using BMIPP and sestamibi scintigraphy. *J Nucl Med.* 1996;37:718–722.

8. Franken PR, Hambye AS, De Geeter FW. BMIPP imaging to assess functional outcome in patients with acute and chronic left ventricular dysfunction. *Int J Card Imaging.* 1999;15:27–34.

9. Knapp FF Jr, Kropp J. BMIPP: design and development. *Int J Card Imaging.* 1999;15:1–9.

10. Nohara R, Hosokawa R, Hirai T, et al. Basic kinetics of 15-(p-iodophenyl)-3-R,S-methylpentadecanoic acid (BMIPP) in canine myocardium. *Int J Card Imaging.* 1999;15:11–20.

11. Nohara R. Lipid metabolism in the heart: contribution of BMIPP to the diseased heart. *Ann Nucl Med.* 2001;15:403–409.

12. Taki J, Matsunari I, Nakajima K, Tonami N. BMIPP compared with thallium redistribution. *Int J Card Imaging.* 1999;15:49–59.

13. Matsunari I, Saga T, Taki J, et al. Kinetics of iodine-123-BMIPP in patients with prior myocardial infarction: assessment with dynamic rest and stress images compared with stress thallium-201 SPECT. *J Nucl Med.* 1994;35:1279–1285.

14. Taki J, Nakajima K, Matsunari I, Bunko H, Takada S, Tonami N. Impairment of regional fatty acid uptake in relation to wall motion and thallium-201 uptake in ischaemic but viable myocardium: assessment with iodine-123-labelled beta-methyl-branched fatty acid. *Eur J Nucl Med.* 1995;22:1385–1392.

15. Nakajima K, Shimizu K, Taki J, et al. Utility of iodine-123-BMIPP in the diagnosis and follow-up of vasospastic angina. *J Nucl Med.* 1995;36:1934–1940.

16. Fujibayashi Y, Nohara R, Hosokawa R, et al. Metabolism and kinetics of iodine-123-BMIPP in canine myocardium. *J Nucl Med.* 1996;37:757–761.

17. Yamamichi Y, Kusuoka H, Morishita K, et al. Metabolism of iodine-123-BMIPP in perfused rat hearts. *J Nucl Med.* 1995;36:1043–1050.

18. Noriyasu K, Mabuchi M, Kuge Y, et al. Serial changes in BMIPP uptake in relation to thallium uptake in the rat myocardium after ischaemia. *Eur J Nucl Med Mol Imaging.* 2003;30:1644–1650.

19. Nishimura T, Sago M, Kihara K, et al. Fatty acid myocardial imaging using ^{123}I-beta-methyl-iodophenyl pentadecanoic acid (BMIPP): comparison of myocardial perfusion and fatty acid utilization in canine myocardial infarction (occlusion and reperfusion model). *Eur J Nucl Med.* 1989;15:341–345.

20. Nohara R, Okuda K, Ogino M, et al. Evaluation of myocardial viability with iodine-123-BMIPP in a canine model. *J Nucl Med.* 1996;37:1403–1407.

21. Mochizuki T, Murase K, Higashino H, et al. Ischemic "memory image" in acute myocardial infarction of ^{123}I-BMIPP after reperfusion therapy: a comparison with ^{99m}Tc-pyrophosphate and ^{201}Tl dual-isotope SPECT. *Ann Nucl Med.* 2002;16:563–568.

22. Hashimoto A, Nakata T, Tsuchihashi K, Tanaka S, Fujimori K, Iimura O. Postischemic functional recovery and BMIPP uptake after primary percutaneous transluminal coronary angioplasty in acute myocardial infarction. *Am J Cardiol.* 1996;77:25–30.

23. Misumi I, Kimura Y, Hokamura Y, Yamabe H, Ueno K. Myocardial rest iodine-123-beta-methyl-iodophenyl-pentadecanoic acid scintigraphy compared with dipyridamole stress thallium-201 scintigraphy in unstable angina. *Intern Med.* 1998;37:21–26.

24. Fukuzawa S, Inagaki M, Morooka S, Inoue T, Sugioka J, Ozawa S. An effective tool to detect lesions causing unstable angina with multivessel disease: iodine-123-betamethyl-p-iodophenyl-pentadecanoic acid single photon emission computed tomography. *J Cardiol.* 1996;28:191–198.

25. Takeishi Y, Chiba J, Abe S, Tonooka I, Komatani A, Tomoike H. Heterogeneous myocardial distribution of iodine-123 15-(p-iodophenyl)-3-R,S-methylpentadecanoic acid (BMIPP) in patients with hypertrophic cardiomyopathy. *Eur J Nucl Med.* 1992;19:775–782.

26. Kurata C, Tawarahara K, Taguchi T, et al. Myocardial emission computed tomography with iodine-123-labeled beta-methyl-branched fatty acid in patients with hypertrophic cardiomyopathy. *J Nucl Med.* 1992;33:6–13.

27. Sloof GW, Visser FC, Bax JJ, et al. Increased uptake of iodine-123-BMIPP in chronic ischemic heart disease: comparison with fluorine-18-FDG SPECT. *J Nucl Med.* 1998;39:255–260.